

ORIGINAL ARTICLE

S. Lausson · G. E. Volle · M. Bourges · E. Pidoux
C. Borrel · G. Milhaud · M. S. Moukhtar
A. Jullienne · F. Treilhou-Lahille

Calcitonin secretion, C cell differentiation and proliferation during the spontaneous development of murine medullary thyroid carcinoma

Received: 23 January 1995 / Accepted: 3 April 1995

Abstract Medullary thyroid carcinoma (MTC), a C cell neoplasm, synthesizes large amounts of calcitonin (CT), its biological marker. However, in some cases with a poor prognosis, MTC is associated with low basal CT levels owing to a decrease in the thyroid CT content. Using a murine model of human MTC, we studied the relationships between CT biosynthesis, C cell proliferation, and the circulating CT level during MTC progression. Cell proliferation was revealed by autoradiography of radioactive thymidine incorporation in dividing nuclei, after CT or CT mRNA detection by immunocytochemistry (ICC) or in situ hybridization (ISH). All rat thyroids showed a severe hyperplasia of C cells containing significant amounts of CT and CT mRNA, and a very low mitotic index. Tumours were found in 68% of the thyroids. In the strongly immunoreactive small nodules (ICC+), many labelled nuclei were observed. Subsequently some nodular cells, still containing detectable CT mRNA (ISH+), were not detected by immunocytochemistry (ICC–) owing to a dramatic decrease in secretory granules. Their mitotic index increased, and a rise of the basal CT plasma level was noted. These ISH+, ICC– tumour MTC cells represent a modified aggressive tumour C cell population exhibiting an increased ability to proliferate and were detected by the rise in the basal circulating CT level.

Key words Rat C cells · Differentiation · Proliferation · Calcitonin · Medullary thyroid carcinoma

Introduction

Human medullary thyroid carcinoma (MTC) [14] is a C cell neoplasm [29] that occurs in spontaneous or familial forms that are dominantly inherited, two of them associated with the development of multiple endocrine neoplasia (MEN2 A and B) [24]. The gene for MTC has been assigned to chromosome 10 [22, 35]. Recently, all these syndromes have been found to be associated with germline mutations of the RET proto-oncogene [12, 17, 26]. For all forms, several successive histopathological steps have been described for the human disease [10, 38], resulting in multifocal intrafollicular micronodules whose growth leads to malignant MTCs. It is thought that the association of cells in micronodules is often preceded by a local C cell hyperplasia [39]. These normal and tumour cells secrete calcitonin (CT), the hypocalcaemic and hypophosphataemic hormone [16] that is the best biological marker of MTC development [25]. Plasma CT levels of suspected patients show an abnormal increase when measured by radioimmunoassay under basal conditions [1, 23, 25] and/or after stimulation by calcium or pentagastrin [15]. However, though CT is the most reliable marker of MTC, its levels reflect secretions of both normal and tumour C cells and do not allow a distinction between the two. Finally, some MTCs are associated with low basal CT plasma levels and a low intra-tumour CT content. These clinical observations are always associated with a poor prognosis of the disease [21, 32, 33], suggesting relationships between modifications of the hormonal production and increased malignancy of the tumour.

We have validated the WagRij strain of rat as a good animal model of human MTC: in the course of ageing, development of a spontaneous MTC that is morphologically very similar to the human disease is seen with a high frequency among these animals [3]. In young

This work was supported by grant no. 6424 from the Association pour la Recherche sur le Cancer to F. Treilhou-Lahille

S. Lausson (✉) · G. E. Volle · F. Treilhou-Lahille
URA 1116 CNRS, Bât. 441, Université Paris-Sud-Orsay,
F-91405 Orsay Cédex, France

M. Bourges
Département de Microscopie Electronique, Faculté de Médecine,
F-63001 Clermont-Ferrand Cédex, France

E. Pidoux · M. S. Moukhtar · A. Jullienne
U.349 INSERM, Centre Vigo-Petersen, 6 rue Guy Patin,
F-75010 Paris, France

G. Milhaud
Service de Médecine Nucléaire, Hôpital Saint-Antoine,
184 rue du Faubourg Saint-Antoine, F-75012 Paris, France

adults, thyroids display a C cell hyperplasia with variable intracellular immunoreactive CT content [19]. The thyroid contents of CT and its messenger RNA are higher than in the original Wistar strain [8]. Finally, these so called pretumour features are genetically transmitted [9]. However, no MEN-like association seems to exist, though other tumours have been described, sometimes with high frequency (pituitary adenomas, 69% of the aged females [2]: the Wag/Rij rat could thus be a model of the third form of familial MTC described by Nelkin et al. [28]. This form is characterized by a late age of onset, and lacks association with MEN-like endocrine or neural lesions. However, unlike this human form of the disease, RET mutations have not been reported.

We have recently reported that, as for the human disease, many cells of the largest tumours are negative for anti-CT antibodies [20]. Therefore, we decided to examine potential relationships between differentiation and proliferation of tumour C cells during the successive histopathological stages of MTC progression and their effect on the basal circulating CT levels. The simultaneous visualization of intracellular CT and of C cell proliferation was achieved using a two-step technique: the specific ISH or ICC characterization of MTC cells with a probe directed against CT, followed, on the same slide, by the autoradiographic detection of a radioactive thymidine in dividing nuclei.

Materials and methods

Rats were raised under conventional conditions in our laboratory. The breeding stock was obtained from the TNO Institute (Rijswijk, The Netherlands).

During the past 2 years, 83 rats of both sexes were killed and their thyroids were examined for CT biosynthesis: 30 were 18 months old and 53 were 24 months old.

Basal CT levels were measured for 67 rats, 30 of which were 18 months old and 37, 24 months old. Blood samples (1 ml) were obtained by retro-orbital sinus puncture under light ether anaesthesia, collected in heparinized tubes and centrifuged at 4°C, and then stored at -20°C until assayed. Calcitonin was measured by our usual procedure [7] using a heterologous assay for human CT cross-reacting totally with murine CT. In brief, a polyclonal anti-human-CT serum (As 732) at a final dilution of 1/200,000 was incubated with ¹²⁵I-labelled hCT in the presence or absence of increasing amounts of synthetic hCT (from 7.8 to 1,000 pg per tube), or samples (50 µl of unextracted plasma). For plasma samples, protein effects were matched by the addition of 50 µl per tube of affinity-stripped control rat plasma. The sensitivity of the assay amounted to 7–10 pg per tube, corresponding to 100 pg per ml of plasma. Synthetic human CT was iodinated by the chloramine-T method to a specific activity of 300 Ci/g. Na¹²⁵I (17 Ci/ng; 1 Ci=37 10¹⁰ Bq) was obtained from Dupont de Nemours-NEN, France. As 732 was raised in the sheep against the unconjugated intact synthetic human molecule (As 6732, J.P.Barlet, INRA, Theix, France).

Injections of tritiated thymidine were administered to 13 of the 53, 24-month-old rats before sacrifice (1 µCi g⁻¹, 3.17 Bq mM⁻¹, NEN Laboratories). Two experiments were performed:

In experiment 1, 5 rats each received one injection of tritiated thymidine i.p., and all were sacrificed 18 h after the injection.

In experiment 2, 8 rats each received four injections of tritiated thymidine i.p./24 h. Animals were sacrificed after lags of 3, 5, 7 and 13 days from the last injection (2 at each time point).

The thyroid glands were removed under a dissecting microscope and processed for histological purposes. They were immersed either in 4% paraformaldehyde in 0.1 M phosphate buffer at pH 7.4 for 1 day at 4°C (experiment 1), or in Bouin's fluid for 3 days at 4°C (experiment 2). All the samples were dehydrated and embedded in paraffin by standard procedures (morphology and ICC) or as previously reported for comparative ICC and ISH [20]. Serial transverse sections 7 µm thick were cut and processed for routine morphological Mann-Dominici staining (toluidine blue-Eosin) or for specific peptide and/or mRNA detection, followed by autoradiography (see below). The absolute number of nuclei per unit of area (mm²) was calculated on sections stained with toluidine blue.

Specific immunodetection of rat CT was performed using anti-human calcitonin antibodies and the PAP procedure, as already described [37]. The anti-calcitonin antiserum As. 6732 was raised in the sheep. The specificity of the reaction was tested using normal sheep serum, or specific antibody saturated with an excess of CT in the first incubating medium.

In situ hybridization was performed as recently described [20]. The CT probe (rCT 37) was a 37mer oligonucleotide complementary to exon 4 of the rat calcitonin gene, corresponding to the 2–14 domain of rat CT amino acid sequence [30]. It was synthesized and purified by GENSET (France). The probe was labelled at the 3' end with digoxigenin (d-UTP-dig, Boehringer, France) using terminal deoxynucleotidyl transferase, according to a protocol already described [20]. The labelled probe was used without purification and could be kept at 4°C for several months.

Autoradiography was performed on the same slides after immunohistochemistry. The slides were acetylated, washed overnight, dehydrated and dipped in NTB2 Kodak nuclear emulsion diluted 1:1 in distilled water. After a 4-week exposure, the slides were developed in Kodak D19, 4 min at 20°C, and fixed for 15 min in a solution of sodium thiosulfate, 30% in distilled water. Occasionally, the slides were counterstained with methyl green.

For electron microscopic observation, the thyroids were perfused with isotonic buffer saline (2 min) and fixed by perfusion in a solution containing 3% glutaraldehyde in 0.1 M cacodylate buffer pH 7.4 (10 min); the lobes were removed under a dissecting microscope and immersed in the same fixative for 30 min at 4°C. The samples were postfixed for 2 h in osmium tetroxide, 1% in the same buffer, dehydrated and embedded in Epon 812. Sections 70 nm thick were routinely stained with uranyl acetate and lead citrate and examined with a JEOL 100B electron microscope. Control 1-µm-thick sections were stained with 1% toluidine blue in borax and observed with light microscopy.

The quantitative analysis of the labelled nuclei was performed using computerized techniques that are conventional in video microscopy. The microscopic image was digitalized and saved as a disk file in the best conditions of illumination and contrast. The image was then processed using the Optilab V 2.01 computer program. The region of interest was delimited under visual control and the area measured in pixels. The results were converted to square millimetres after standardization with a Malassez cell. The number of labelled nuclei was determined on the digitalized image in the defined region of interest.

All data were subjected to variance analysis, and comparisons between two means were made using the Dunnett's *t*-test. Relations between two variables were studied using the Snedecor and Cochran correlation test [36].

Results

Principal C cell abnormalities of the old Wag/Rij rat thyroid: modifications of calcitonin expression.

The histopathological tissue structure was studied in the 83 thyroids removed from rats 18 and 24 months old.

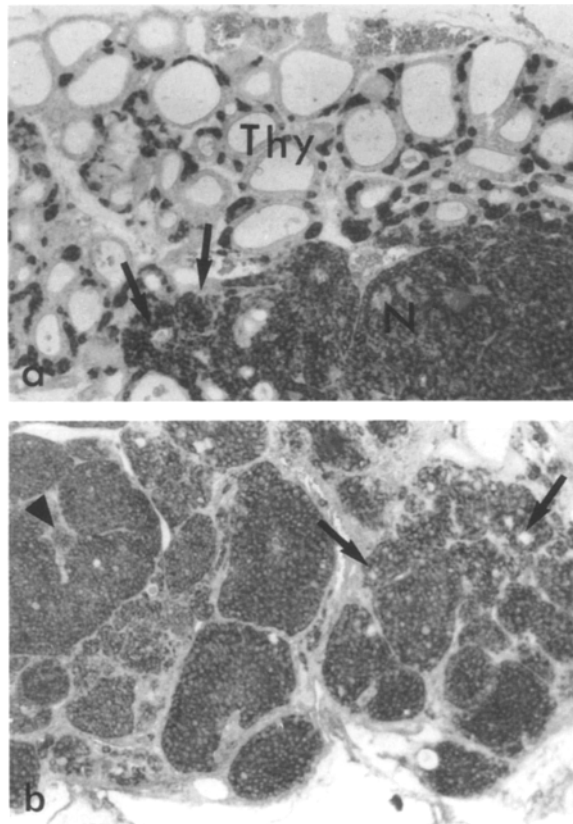


Fig. 1a–c Calcitonin (CT) detection by the in situ hybridization (ISH) method in diffuse and nodular hyperplastic C cells, and in medullary thyroid carcinoma (MTC) cells. No counterstain, 60. **a** General overview of a thyroid lobe of an aged (24-month-old) Wag/Rij rat. All C cells are specifically detected by the alkaline phosphatase activity tagged on the anti-digoxigenin antibody. The right side shows the severe diffuse hyperplasia in the thyroid tissue (*Thy*). A multifocal nodule is seen on the left side (*N*). Arrows focus on hyperplastic thyroid follicles in the course of being included in the nodule. **b** Overview of a medullary carcinoma. All the MTC cells are detected by ISH using a CT probe. There is no remnant of thyroid tissue, but thyroid follicles are still apparent in the middle of large bulks of MTC cells (*arrows*). **c** Same tumour, corresponding area in the adjacent section, examined by ISH using a CGRP probe. Same staining pattern as above, but the stain is fainter though performed simultaneously under the same conditions

Diffuse C cell hyperplasia

Both lobes of all the thyroids displayed a severe diffuse hyperplasia, which is regarded as normal in aged rats. The numerous C cells were located intrafollicularly, close to the basal lamina, and often organized in a complete peripheral layer. They contained large amounts of both immunoreactive CT and its messenger RNA (Figs. 1a, 2a, b).

Tumours

Many (68.7%) of the thyroids also harboured C cell masses, varying in size between 50 and 5,000 μm . All

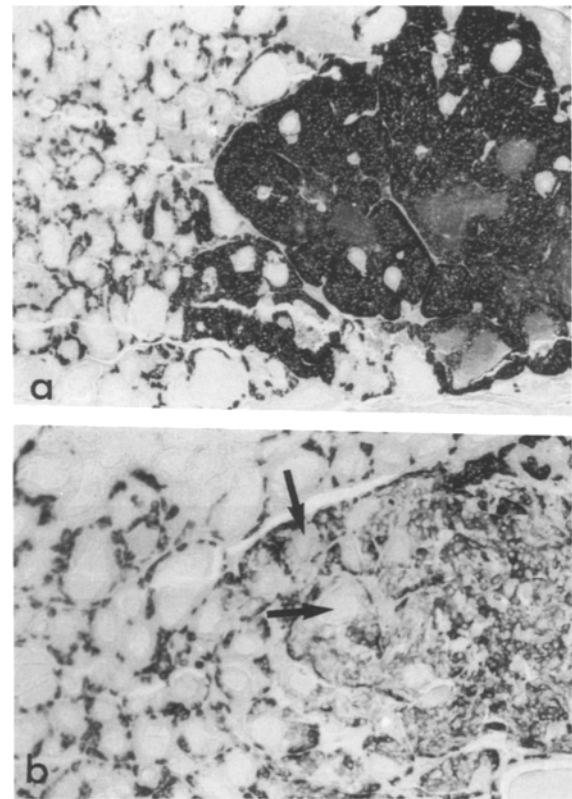
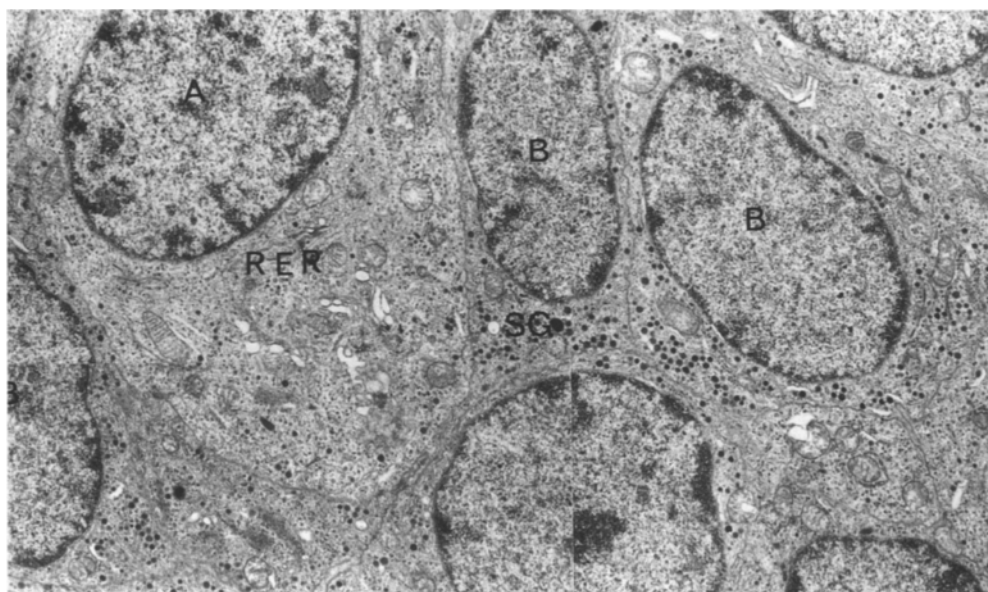


Fig. 2a, b Immunoreactivity of two nodules of the same size (700 μm maximal diameter). As 6732 and PAP-Nickel procedure, no counterstain, ($\times 60$) **a** All diffuse and nodular C cells are strongly immunoreactive. The follicular structure is apparent all over the nodule. Basal CT level: 200 pg/ml. **b** As **a**, except that the immunoreactivity of the nodular cells is variable. The centre of the nodule looks completely disorganized, with the follicular structure confined to the periphery (*arrows*). Basal CT level: 600 pg/ml

the tumour C cells contained large amounts of CT mRNA, which were detected by ISH with a CT probe (Fig. 1a, b).

In contrast to the homogeneous ISH stain, the ICC stain was heterogeneous. The immunonegative cells that we have already described in large MTCs [20] were observed in tumours as small as 300 μm , and their number increased during tumour development (Fig. 2b). The tumours were thus classified into two groups, nodules and MTCs, on the basis of both histological criteria and pattern of immunoreactivity after ICC with anti-CT antibodies: (i) In the so-called nodules (42%), the follicular structure of the thyroid was preserved and the strongly immunoreactive C cells were still enclosed in the basal lamina of the thyroid follicle. Most (79%) were smaller than 400 μm , while the largest had a maximal diameter of 700 μm . (ii) In contrast, MTCs were characterized by a variable tissue structure: though some immunoreactive follicles were still present at the periphery of the tumour, a largely immunonegative centre displayed a disorganized aspect owing to the destruction of the basal laminae and the fusion of the enlarged follicles. The tumour mass, wrapped in a dense layer of connective tissue, was

Fig. 3 Fine structure of both types of tumour cells. General overview of a tumour area, achieved by combining four original micrographs, showing variable densities of secretory granules (SG). A cell almost devoid of this compartment (A) is surrounded by cells with an apparently normal endocrine phenotype (B). However, the pre-Golgi (RER) and the Golgi (GA) compartments are conspicuous. Routine stain, $\times 4,000$



finally invaded by capillaries. Many (70%) were larger than 400 μm in diameter. The fine structure of the immunonegative cells was characterized by a dramatic secretedecrease in the number of secretory granules that usually store the secreted peptides (Fig. 3), explaining the loss of CT immunoreactivity.

The frequencies of the abnormalities described above are reported in Table 1, lines 1 and 2; no sex difference was noted. In lines 3, 4, and 6 the morphology and the CT biosynthetic parameters of the hyperplastic, nodular and MTC cells are summarized.

Effects of the pathological thyroid status on basal CT plasma levels (Table 1, line 5)

Diffuse hyperplasia (n=23)

The mean value was 647 ± 146 pg/ml, which was taken as the normal value for aged rats.

Immunoreactive nodules (n=22, size range 50–700 μm)

The mean value was 466 ± 113 pg/ml, not significantly different from that in hyperplasia. Furthermore, the CT levels were not correlated with tumour size.

Heterogeneously stained MTCs (n=20, size range 500–5,000 μm)

These were all associated with a rise of basal CT plasma levels to a mean value of $2,800 \pm 652$ pg/ml, significantly different from those in both diffuse hyperplasia and immunoreactive nodules ($P=0.0001$). The basal CT levels were closely correlated with the size of MTCs ($r=0.627$, $P=0.003$). Furthermore, when only the small MTCs

Table 1 Frequencies, morphology, CT biosynthetic variables and proliferative ability of the C cell abnormalities of the old Wag/Rij rat

	Hyperplasia	Nodules	MTCs	
Animals	18 m. 24 m.	37% 28%	53% 15%	10% 57%
Tissue structure	Diffuse	C cell masses		
		50 to 700 μm	300 to 5000 μm	
ISH	+	+	+	
Basal CT plasma levels	Low	Low	High	
ICC	+	+	+	–
Mitotic index	Low	High	High	High
Mitotic rate	Slow	Slow	Slow	Rapid

(<1,500 μm) were considered, the mean value ($1,694 \pm 513$ pg/ml; $n=14$) remained significantly different from that for immunoreactive nodules (466 ± 113 pg/ml; $n=22$).

Proliferative ability and division rate of hyperplastic and tumour C cells

C cell differentiation and proliferation were detected consecutively on the same section. In both experiments, the diffuse hyperplastic cells displayed only a few heavily labelled nuclei, preferentially located close to a nodular area (Fig. 4a). All the nodules, even those that were small and strongly immunoreactive, showed numerous directly labelled nuclei (Fig. 4a). This number was obviously increased in the immunonegative areas of large MTCs (Fig. 4b).

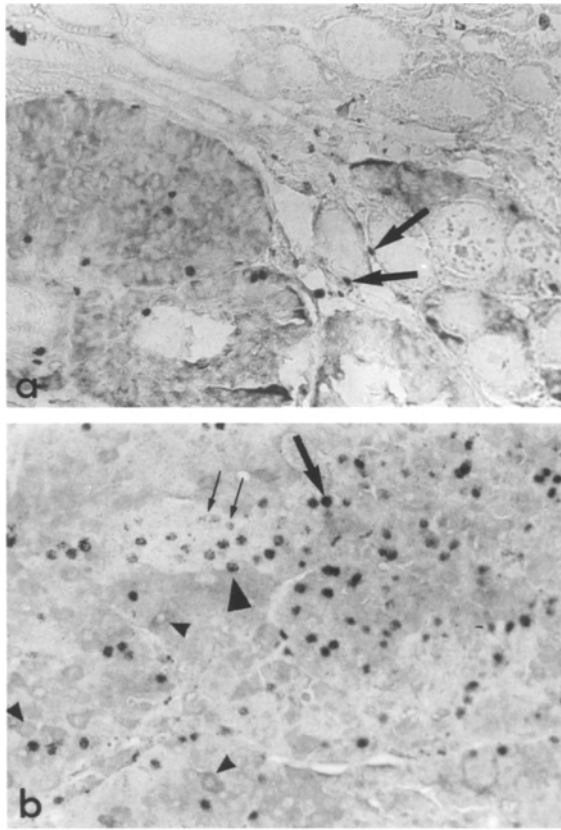


Fig. 4 a, b Autoradiographic labelling of dividing nuclei. **a** Overview of a thyroid lobe showing diffuse and nodular hyperplastic cells detected by the immunoperoxidase technique with nickel omitted, followed by autoradiography. Lag-time 3 days, $\times 150$. Note the heavily labelled nuclei at the periphery of two hyperplastic follicles. *Arrows* focus on labelled nuclei in the diffuse tissue located close to the nodule. **b** Intense proliferation in a large MTC. The major part of the labelling is located in unstained cells. Same technique and lag-time as in **a**, $\times 150$

Experiment 1

The 5 rats were sacrificed 18 h after a single injection of the radioactive tracer; the labelled nuclei underwent only one mitotic cycle. Five ICC+ tumours and 1 heterogeneously stained MTC were available. In immunoreactive tumours and in the ICC+ areas of the large MTC, the total number of labelled nuclei was $56 \pm 11 \text{ mm}^{-2}$, representing 1% of total nuclei, with no significant difference attributable to tumour size. In fact, it was significantly higher in the ICC- areas of the large MTC, with $115 \pm 1 \text{ mm}^{-2}$ ($P < 0.01$), representing 1.8% of the total nuclei.

Experiment 2

The 8 rats were sacrificed at four different times after the injections, in an attempt to evaluate the mitotic rate. The number of mitotic cycles undergone by a given nucleus since the moment of the last injection was indicated by its density of labelling: $n/2$ after the first division, $n/4$ after the second one, and $n/8$ after the third

Table 2 Thyroid abnormalities observed after each latency period in experiment 2

	Latency (days)			
	3	5	7	13
Diagnosis	Nodule Nodule	Carcinoma Carcinoma	Carcinoma Nodule	Carcinoma Nodule

Table 3 Number of labelled nuclei per square millimeter in each mitotic cycle. Comparative values in small immunoreactive tumours (nodules) and in a large heterogeneous MTCs

No of cycle	Latency			
	7 Days		13 Days	
	Nodule	Carcinoma	Nodule	Carcinoma
n1	58 ± 4	71 ± 13	83 ± 13	82 ± 17
n2	69 ± 14	132 ± 13	21 ± 4	199 ± 44
	$P = 0.01$		$P < 0.01$	
n3	8 ± 5	47 ± 7	2 ± 2	127 ± 23
	$P < 0.005$		$P < 0.001$	

one. The $n/8$ labelling of the 4th division could not be distinguished from the general background. The histopathological diagnosis for each latency is reported in Table 2.

In the smallest nodules observed, which were all totally immunoreactive, the number of labelled nuclei was high, 132 ± 13 ($n=4$), representing 2.1% of total nuclei. It was quite stable in the four nodules, though they were removed at different times after the injections, suggesting that the probability of an immunoreactive cell's undergoing mitosis is the same however many mitotic cycles it has undergone. The twofold increase compared with experiment 1 was due to the four injections of the tracer instead of one.

In larger tumours, strongly and faintly stained areas were estimated separately (respectively ICC+ and ICC-). The number of labelled nuclei in ICC+ areas was 147.6 ± 16.0 for two MTCs, which is not significantly different from the estimation made for the nodules described above. The number was significantly higher in the ICC- areas: 396.6 ± 54.7 for 4 MTCs ($P < 0.05$; Fig. 4 b), a value that did not depend on the latency before sacrifice. It represented a larger fraction of total nuclei, 6.3%.

At both 7 and 13 days after injections, a nodule and a carcinoma were available; the mitotic rates of these pathological stages were compared by evaluating the number in each cycle separately. Data are reported in Table 3. In both cases, the number of heavily labelled nuclei (one mitotic cycle) was roughly identical, confirming data reported above. However the number of nuclei that underwent two and, notably, three, cycles were increased in ICC- areas of carcinomas. Therefore, the high number of labelled nuclei in MTCs was due to a more rapid rate of division.

Taken together, these data suggest that ICC+ and ICC- cells behaved as two homogeneous populations differing in two negatively correlated variables, the mitotic index and the immunoreactivity, indicating the importance of the hormonal storage. They also show that, during MTC development, the ICC- areas, in which the cells divide rapidly, should grow more rapidly than areas ICC+, as is in fact almost always observed in large MTCs.

These results are summarized in Table 1, lines 7 and 8.

Discussion

The three specific stages of MTC progression that we found in the old Wag/Rij thyroid are remarkably similar to the histopathological changes occurring in the familial form of the human disease [10, 38, 39]. All the Wag/Rij thyroids, both sexes, showed a severe diffuse C cell hyperplasia, that can thus be considered as normal for old rats. Besides diffuse hyperplasia, C cell tumours were found in 68.7%, a higher frequency than in the two other strains of rats already studied [11, 13]. However, a significant number of the 2-year-old rats did not develop any tumour, though the whole 3-month-old population shows the pretumour characters established for the human MTC [4, 8, 9, 19]. In the human disease, two different germline mutations of the proto-oncogene RET have been found, one associated with MEN2B, and the other with MEN2A and the familial "MTC only" [12, 26], both of which are regarded as predictive of MTC development in family members at risk. If they exist in the rat model, our data suggest that these germ-line mutations alone would not be able to provoke a tumour, though very recently, the altered RET genes have been shown to be transformant in NIH 3T3 [34]. They also suggest that the predictive value of the pretumour features, including the recent genetic markers, might be questionable for this form of the disease, or that these features might be too limited in extent.

Data obtained after ISH with a CT probe expand our previous report [20]. We show here that, in tumours of all sizes, almost all the cells contained detectable amounts of CTmRNA. ISH with a CT probe is thus the most accurate way of detecting a C cell tumour, in rats as in humans [5]. In contrast, ICC revealed a sub-population of tumour cells unstained with anti-CT antibodies. In the Wag/Rij rat, this loss of hormonal stores occurred in all the tumours, at any moment of their development. We have already reported such an alteration of the CT storage in some diffuse hyperplastic cells during the pretumour period of the young Wag/Rij rat [19]. The same defect has also been depicted in human MTCs [10] and in rat [40] and human [28] MTC cell lines. These data suggest that routine anatomopathological detection of the tumour by the ISH procedure would be more accurate than using ICC, as this procedure detects all MTCs, even the most aggressive cases.

We show here that the loss of immunoreactivity was associated with the dramatic decrease of the secretory

granules in which the mature peptides are classically packaged. The decrease of the granules could be generated by changes affecting the aggregation of CT in the *trans* Golgi network (TGN), including the structure of the peptide itself [6, 18]; however, neither in vitro nor in vivo studies revealed any modification in the post-translational maturation of the CT promolecule. It might better be imputed to modifications of the mechanisms of vesicular budding from the TGN [31]: after infection of a human MTC cell line with the mutated viral small G-protein v-Ha-ras, the presence of numerous secretory granules and a slower proliferation have been reported [27]. Finally, the relative number of immunoreactive nodules decreased with age, while the number of MTCs increased. Therefore, this intracellular modification of the endocrine secretory pathway seems to be a necessary step in the growth of C cell tumours.

The lack of the post-Golgi compartment of storage apparently induced an abnormally elevated basal circulating CT level. This rise could thus be considered as a good marker of dedifferentiation of the tumour cells in this model. This observation seems in complete disagreement with data reported for patients bearing an immunonegative tumour associated with abnormally low basal CT levels. However, in these human cases, the CT mRNA content of the MTC cells has not been investigated, and thus a lack of expression of the CT gene cannot be excluded.

Results of a simultaneous study of C cell proliferation and differentiation suggest that two consecutive events occur during C cell neoplasia: First, a local rise of the mitotic index in several immunoreactive C cells represents the initial, non-inherited stage in the progression towards medullary carcinoma. It affects differentiated C cells, excluding a possible stem cell lineage. Second, there is a loss of CT immunoreactivity, coexisting with a higher mitotic index in a growing fraction of nodular cells, principally due to the presence of shorter mitotic cycles (numerous labelled nuclei, 2nd and 3rd cycles). Extrapolating this to human MTCs, in which the decrease of immunoreactivity has often been associated with a greater malignancy [21, 32-33], we propose that analysis of tumours with ICC and ISH procedures could both warrant the diagnosis of the disease and predict the growth rate of the nodules.

Acknowledgements We wish to thank G. Johannin (Service Commun d'Imagerie, Université Paris-Sud, Orsay) for expert advice and L. Elu for the illustrations.

References

1. Block MA, Jackson CE, Tashjian AHJ (1972) Medullary thyroid carcinoma detected by serum calcitonin assay. *Arch Surg* 104: 579-580
2. Boorman GA, Hollander CF (1973) Spontaneous lesions in the female WAG/RIJ (Wistar) rat. *J Gerontol* 28: 152-159
3. Boorman GA, Van Noord MJ, Hollander CF (1972) Naturally occurring medullary thyroid carcinoma in the rat. *Arch Pathol* 94: 35-41

4. Bouizar Z, Rostène W, Treilhou-Lahille F, Pidoux E, Milhaud G, Moukhtar MS (1987) Early spontaneous deficiency of calcitonin renal binding sites in rats with a high incidence of calcitonin-secreting tumors (Wag/Rij). *Cancer Res* 47: 3595–3598
5. Boultonwood J, Wynford-Thomas D, Richards GP, Craig RK, Williams ED (1990) In-situ analysis of calcitonin and CGRP expression in medullary thyroid carcinoma. *Clin Endocrinol* 33: 381–390
6. Chanaat E, Huttner WB (1991) Milieu-induced, selective aggregation of regulated secretory proteins in the *trans*-Golgi network. *J Cell Biol* 115: 1505–1519
7. Cressent M, Bouizar Z, Moukhtar MS, Milhaud G (1981) Effect of ovariectomy on circulating calcitonin levels in the rat. *Proc Soc Exp Biol Med* 166: 92–95
8. Delehay MC, Cohen R, Segond N, Pidoux E, Treilhou-Lahille F, Milhaud G, Moukhtar MS (1989) Rats developing spontaneously medullary thyroid carcinoma have abnormally elevated levels of calcitonin mRNA. *Biochem Biophys Res Commun* 2: 528–535
9. Delehay MC, Bouizar Z, Pidoux E, Segond N, Treilhou-Lahille F, Milhaud G, Moukhtar MS (1990) Genetic origin of increased calcitonin mRNA levels in rats with high incidence of C cell tumours. *Biochem Biophys Res Commun* 167: 232–237
10. DeLellis RA, Nunnemacher G, Wolfe HJ (1977) C-cell hyperplasia, an ultrastructural analysis. *Lab Invest* 36: 237–248
11. DeLellis RA, Nunnemacher G, Bitman WR, Gagel RF, Tashjian AHJ, Bloun M, Wolfe HJ (1979) C-cell hyperplasia and medullary thyroid carcinoma in the rat. An immunohistochemical and ultrastructural analysis. *Lab Invest* 40: 140–154
12. Doniskeller H, Dou SS, Chi D, Carlson KM, Toshima K, Lairmore TC, Howe JR, Moley JF, Goodfellow P, Wells SA (1993) Mutations in the RET proto-oncogene are associated with MEN 2A and FMTC. *Hum Mol Genet* 2: 851–856
13. Giscard-Darteville S, Pidoux E, Jullienne A, Volle GE, Rostène W, Milhaud G, Moukhtar MS, Bouizar Z (1992) Renal calcitonin receptors in the ageing rat. *Arch Gerontol Geriatr* 15: 101–113
14. Hazard JB, Hawk WA, Crile G (1959) Medullary (solid) carcinoma of the thyroid. A clinicopathological entity. *J Clin Endocrinol Metab* 19: 152–161
15. Hennessy JF, Gray TK, Cooper CW, Ontje DA (1973) Stimulation of thyrocalcitonin secretion by pentagastrin and calcium in two patients with medullary carcinoma of the thyroid. *J Clin Endocrinol Metab* 36: 200–203
16. Hirsch PF, Gauthier GF, Munson PL (1963) Thyroid hypocalcemic principle and recurrent laryngeal nerve injury as factors affecting the response to parathyroidectomy in rats. *Endocrinology* 73: 244–252
17. Hofstra RMW, Landsvater RM, Ceccherini I, Stulp RP, Stelwagen T, Luo Y, Pasini B, Hoppener JWM, Vanamstel HKP, Romeo G, Lips CJM, Buys CHCM (1994) A mutation in the RET proto-oncogene associated with multiple endocrine neoplasia type-2B and sporadic medullary thyroid carcinoma. *Nature* 367: 375–376
18. Kelly RB (1991) Secretory granules and synaptic vesicles formation. 3: 654–660
19. Khattab M, Pidoux E, Volle GE, Bouizar Z, Calmettes C, Milhaud G, Moukhtar MS, Treilhou-Lahille F (1989) Early calcitonin hypersecretion and C cell hyperplasia in rats with high incidence of C cell tumor. *Bone Miner* 6: 249–260
20. Le Guellec P, Dumas S, Volle GE, Pidoux E, Moukhtar MS, Tre-Lahille F (1993) An efficient method to detect calcitonin mRNA in normal and neoplastic rat C cells (medullary thyroid carcinoma) by in situ hybridization using a digoxigenin labeled synthetic oligodeoxynucleotide probe. *J Histochem Cytochem* 41: 389–396
21. Lippman SM, Mendelsohn G, Trump DL, Wells SA, Baylin S (1982) The prognostic and biological significance of cellular heterogeneity in medullary thyroid carcinoma: a study of calcitonin, L-DOPA decarboxylase and histaminase. *J Clin Endocrinol Metab* 54: 233–240
22. Mathews CGP, Chin KS, Easton DF, Thorpe K, Carter C, Liou GI, Fong SL, Bridges CDB, Haak H, Nieuwenhuijzen Kruseman AC, Schifter S, Hansen HH, Telenius HMT-B, Ponder BAJ (1987) A linked genetic marker for multiple endocrine neoplasia type 2A on chromosome 10. *Nature* 328: 527–528
23. Melvin KEW, Miller HH, Tashjian AHJ (1971) Early diagnosis of medullary carcinoma of the thyroid gland by means of calcitonin assay. *N Engl J Med* 285: 1115–1120
24. Melvin KEW, Tashjian JR, AH, H. MH, (1972) Studies in familial (medullary) thyroid carcinoma. *Recent Prog Hormone Res* 28: 399–470
25. Milhaud G, Tubiana M, Parmentier C, Coutris G (1968) Epithélioma de la thyroïde sécrétant de la thyrocalcitonine. *CIR Acad Sci [D] (Paris)* 266: 608–610
26. Mulligan LM, Eng C, Healey CS, Clayton D, Kwok JBJ, Gardner E, Ponder MA, Frilling A, Jackson CE, Lehnert H, Neumann HPH, Thibodeau SN, Ponder BAJ (1994) Specific mutations of the RET proto-oncogene are related to disease phenotype in Men 2A and FMTC. *Nature [Genetics]* 6: 70–74
27. Nakagawa T, Mabry M, Bustros de A, Ihle JN, Nelkin B, Baylin SB (1987) Introduction of v-Ha-ras oncogene induces differentiation of cultures of human medullary thyroid carcinoma cells. *Proc Natl Acad Sci USA* 84: 5923–
28. Nelkin BD, Bustros de A, Mabry M, Baylin SB (1989) The molecular biology of medullary thyroid carcinoma. A model for cancer development and progression. *JAMA* 261: 3130–3135
29. Pearse AGE (1968) Common cytochemical and ultrastructural characteristics of cells producing polypeptides hormones (APUD series) and their relevance to thyroid ultimobranchial C cells and calcitonin. *Proc R Soc Lond B Biol Sci* 170: 71–80
30. Raulais D, Hagaman J, Ontjes D, Lundblatt RL, Kingdom HS (1976) The complete amino-acid sequence of rat thyrocalcitonin. *Eur J Biochem* 64: 607–
31. Rothman JE, Orci L (1992) Molecular dissection of the secretory pathway. *Nature* 355: 409–416
32. Ruppert JM, Eggleston JC, Bustros de A, Baylin SB (1986) Disseminated calcitonin-poor medullary thyroid carcinoma in patient with calcitonin-rich primary tumor. *Am J Surg Pathol* 10: 513–518
33. Saad MF, Ordonez NG, Guido JJ (1984) The prognostic value of calcitonin in medullary carcinoma of the thyroid. *J Clin Endocrinol Metab* 59: 850–856
34. Santoro M, Carlomagno F, Romano A, Bottaro DP, Dathan NA, Grieco M, Fusco A, Vecchio G, Matoskova B, MH K, Di Fiore PP (1995) Activation of RET as a dominant transforming gene by germline mutations of MEN2A and MEN2B. *Science* 267: 3821–383
35. Simpson NE, Kidd KK, Goodfellow PJ, McDermid H, Myers S, Kidd JR, Kackson CE, Duncan AMV, Farrer LA, Brasch K, Castiglione C, Genel M, Gertner J, Greenberg CR, Gusella JF, Holden JJA, White BN (1987) Assignment of multiple endocrine neoplasia type 2A to chromosome 10 by linkage. *Nature* 328: 528–530
36. Snedecor G, Cochran W (1967) Statistical methods. The Iowa State University Press,
37. Treilhou-Lahille F, Cressent M, Taboulet J, Moukhtar MS (1979) Immuno-histochemical staining of mouse C cells during postnatal histogenesis of the thyroid. *Histochemistry* 63: 69–80
38. Williams ED (1966) Histogenesis of medullary carcinoma of the thyroid. *J Clin Pathol* 19: 114–119
39. Wolfe HJ, Melvin KE, Servi-Skinner SJ, Al Saadi AH, Juliar JF, Jackson CE, Tashjian AHJ (1973) C-cell hyperplasia preceding medullary thyroid carcinoma. *N Engl J Med* 289: 437–441
40. Zeitinoglu FS, DeLellis RE, Gagel RF, Wolfe HJ, Tashjian AH (1980) Establishment of a calcitonin-producing rat medullary thyroid carcinoma cell line. I. Morphological studies of the tumor and cells in culture. *Endocrinology* 107: 509–515